Development of a Leg and Foot Model with Ground Contact for Analysis and Simulation of Human Gait

João Vasco Couto Amorim Marques
joaoamorimmarques@tecnico.ulisboa.pt

Instituto Superior Técnico, Lisboa, Portugal

June 2015

Abstract

The correct calculation of foot and ground contact forces and their application points is a crucial and indispensable step in path planning or human movement simulation. The purpose of this work is the development of a computational model of the human leg and foot that, using forward dynamic analysis with natural coordinates, accurately calculates the contact forces and its application points generated during the contact between the foot and the floor in level walking.
The contact detection algorithm and contact force model were implemented in the multibody dynamics code Apollo in a forward and inverse dynamics perspective. A contact force law with a moderated coefficient of restitution is used to simulate the soft tissue contact with the ground of a leg and foot multibody model described with four anatomical segments. Contact detection is assured through the use of an iterative method that recurs to implicit surfaces, in particular planar, quadric and superquadric surfaces, to find possible contact pairs. The model was tested for simple test cases.
With the purpose of correctly calculate the contact forces, an optimization process was implemented to find the best values for the size, position and orientation of the surfaces used to define the sole of the foot. The forces obtained through the contact force model with the values determined by the optimization were compared with experimentally measured values to evaluate the effectiveness of the optimization process.

Keywords: Contact detection, Multibody dynamics, Foot force, Implicit surfaces, Movement simulation, Contact forces

1. Introduction

The human body, as well as its movement, have been studied for a long time. From ancient Greece (600 B.C. - 200 A.D) to the twentieth century, the search for knowledge of the human body had many contributors, from Pythagoras, Hippocrates, Aristotle and many others to A. V. Hill. In the early seventies, the term biomechanics was approved by the scientific community to describe the study of the mechanical principles that rule living organisms [1].

Nowadays the study of human movement is still of great relevance and it has application in various fields: sports medicine, in order to improve performance and prevent injury [1–3], to design and test sport equipment [4], to determine pathologies associated with human movement or posture, to correctly design prostheses and orthoses [2], between other applications. The correct calculation of contact and associated forces can have a great impact in most of those applications.

The purposes of this work is to develop and implement an efficient contact detection algorithm and an all purpose contact force model that could correctly calculate the ground reaction forces during human movement. For that it is required some basic understanding of the concepts involved in contact detection, contact force models and friction models.

To achieve objective of this work the correct approximation of the human foot, using implicit surfaces, to a bimechanical model of the leg and foot made of four segments [5] is needed, so that the ground reaction forces obtained are the closes possible to the experimentally obtained. For that, a review of relevant concepts and models is important.

1.1. Contact Detection

Rigid body contact, which can be defined as the sharing of the same physical space by two different bodies or objects, generating forces opposing body intersection [6], has various applications in computational physics and is an important step in mechanical modelling [7, 8]. It is of even

greater relevance in forward dynamic simulations [9].

In a general sense, the modulation of rigid body contact can be divided in multiple steps: $i)$ definition of the geometric constraints that define the bodies, $ii)$ detection of possible contact bodies, areas or points, $iii)$ application of the correct constitutive force laws [10–12].

Contact detection is one of the most difficult and challenging parts of mechanical simulation [10, 13]. It is also one of the more computationally expensive processes involved, increasing it's demands as the complexity of the objects increase [14, 15].

In the last few years many different algorithm were proposed with the objective of decreasing the demands of contact detection. It is, however, common to reduce the number of bodies that have to be tested for contact in each time step or configuration by using bounding volumes or boxes [14, 15] and as such, reducing computational time [12]. These could be the so called broad-phase or pre-search algorithms, whereas methods that investigate further if there is contact can be called narrow-phase or detailed search algorithms [7, 8].

In the present work (super)ellipsoids are used, but not as bounding volumes but as contact surfaces as proposed by Lopes et al. [6], where contact detection is based in the common normal concept [16]. In this method, the contact detection problem is reduced to determine a pair of points and respective normals and evaluate their collinearity. The detection of the correct contact candidate points is highly efficient, using the Newton-Raphson method, as it only requires a few number of iterations to find an accurate solution [17].

1.2. Contact Forces

A key point in contact-impact interactions is the constitutive force law utilized [18]. Force based models, also known as penalty models, have the advantage of being simple and effective [18] and being able to easily approximate body deformation [8, 19]. However, for this kind of methods is sometimes difficult to choose the right model and parameters, since the geometry of the contacting bodies and nature of the materials involved play a very significant role in the modelling of the contact process [18, 20].

The development of force models is mainly made based on the Hertz law joined together with a damping factor, in order to consider the energy dissipation that occurs during contact events [18, 21].

$$F = K\delta^n + D\dot{\delta} \tag{1}$$

where K is the relative contact stiffness, δ represents the indentation, n the non-linear exponent , D is the damping factor and $\dot{\delta}$ represents the indentation velocity.

Different approximations of the damping factor lead to different force models and the selection of the model has a strong impact on the prediction of dynamic behaviour [18]. It is important to refer that these models are typically a function of the coefficient of restitution, which is the ratio between the post- and pre-impact velocities [18, 21].

In this work we use model proposed by Flores et all. [21]. This has the particularity of performing well for medium and low coefficient of restitution values and can be easily included in the equations of motion of multibody systems [21].

1.3. Friction Force

Friction is a phenomena existent in the physical interface of bodies in contact. It is a highly complex and non-linear phenomena. In order to correctly model friction one has to take into consideration various parameters and an accepted generalized model does not exist [22, 23]. There are various different models present in the literature [23].

A well accepted division regarding friction models is between static friction models and dynamic friction models. The former are valid for low tangent velocities between the bodies in contact whilst the latter are used when high velocities are expected [22, 24]. The purpose of this work is to study and modulate the foot-ground contact during gait. As in gait the foot-ground tangential velocities during contact can be considered small [25], only static models seem to be appropriate.

In terms of static friction models, the most simple and probably most important and used model is the Coulomb friction model [22, 26], where the friction force is proportional to the normal load:

$$F_{Coulomb} = \mu F_N \tag{2}$$

where μ is called Coulomb friction coefficient.

The model implemented in this work consists on the sum of the Coulomb friction term with a viscous friction term, that depends on the tangent velocity [27].

1.4. Foot Models

The human foot is a mechanical structure of high complexity [28]. However, in many biomechanical studies the foot is considered to be a single rigid body [27]. Previous approaches did not even consider the foot as a rigid body and would fix it to the ground during the stand phase, which in some ways limited the movement [27, 29].

Over the years various biomechanical models for the foot (and leg) were proposed, being of relevance the ones proposed by Melgan [30], Gilchrist and Winter [29], Jenkyn and Nicol [31], Moreira [27] and Vilà [32].

In this work, the biomechanical model used was proposed by Malaquias [5], and consists of four segments and four joints and in total it presents thirteen degrees of freedom.

1.5. Optimization

Since the human foot is highly complex, and due to the fact that is different for almost every one, there is no set of surfaces fit to every foot. And because the various surfaces

distributed in the sole of the foot can be different form each other, there is no set of values that fit all the surfaces for a single foot. For that reason, there is need to determine correctly these values so that the forces calculated by the model can be the closer to the ones that are actually applied. In order to find those values, an optimization process was implemented and used.

An optimization problem can be defined as the process used to find the "best" solution for a mathematically defined problem, for which more that one solution is possible (33).

Generally, an optimization problem can be described mathematically as the minimization or maximization of a function, subject to constraints in its variables:

$$\min_{\boldsymbol{x}\in\mathbb{R}^n} f(\boldsymbol{x}) \text{ subject to } \begin{cases} c_i(\boldsymbol{x}) < 0 \\ c_j(\boldsymbol{x}) = 0 \\ \boldsymbol{lb} < \boldsymbol{x} < \boldsymbol{ub} \end{cases} \quad (3)$$

where f is the the function that defines the objective of the problem, $\boldsymbol{x}$ is the set of variables and n the number of variables of the problem. c_i, c_j represent the inequality and equality constraints of the problem and $\boldsymbol{lb}$ and $\boldsymbol{ub}$ represent the lower and upper bounds of the values that $\boldsymbol{x}$ can take in the problem (34).

In this work the approach used for the optimization problem used changed throughout the work and the reasons and changes will be described further on.

2. Methods

In this section the algorithms and models used for the implementation will be described, as well as the foot biomecahinical model used.

2.1. Biomechanical Foot Model

The model used in this work for gait analysis is defined by four segments, which are: leg, rear-foot, mid/fore-foot and toes. Joining this four segments, four joints are considered: talocrural joint, talocalcaneal or subtalar joint, midtarsal or Chopart's joint and metatarsophalangeal joint.

Over all, the model presents a total of thirteen degrees of freedom that are specified in table 1. Figure 1 shows a representation of the axis of those degrees of freedom.

Table 1: Degrees of freedom of foot model [5]

Joint Name	Motion (DOF)
Talocrural joint	Medial/Lateral Rotation (1) Flexion (2)
Talocalcaneal or subtalar	Inversion/Eversion (3)
Midtarsal or Chopart's	Abducton/Adduction (4) Flexion(5) Internal Rotation (6)
Metatarsophalangeal	Flexion(7)

The remaining degrees of freedom (8 to 13) are associated with rotations and translation of the body as a hole.

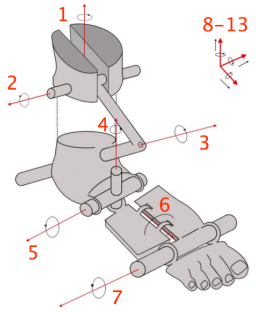

Figure 1: Representation of the axis of the degrees of freedom of foot model [5]

All the information necessary for the implementation of this model (center of mass position, length, mass and inertia moments for each segments) was calculated according with what was described in the work of Malaquias [5].

In terms of surfaces for representing the foot, five surfaces were considered: one for the rear foot, two for the mid-foot and two for the toes. This distribution was made based on an analysis of a pressure distribution over the foot during gait.

2.2. Contact detection

In this chapter the computational method implemented for the modulation of contact will be described. The contact detection was made by using the method developed by Lopes *et al.* [6]. This method can be used for any surface that can be described implicitly and it is, at least, C^2 continuous. It has also been described as a very efficient method [35].

In the contact detection problem, the Newton-Raphson method was used to find a pair of points, belonging to the surfaces considered for contact, with collinear normals n_i and n_j. Collinearity between the distance vector $\boldsymbol{d}_{ij}$ (connecting both candidate contact points represented in figure 2) and the surfaces normal vectors in the candidate contact points is also required. When written mathematically, the conditions are:

$$\boldsymbol{n}_i \times \boldsymbol{n}_j = \boldsymbol{0} \quad (4)$$

$$\boldsymbol{d}_{ij} \times \boldsymbol{n}_i = \boldsymbol{0} \quad (5)$$

$$\boldsymbol{d}_{ij} \times \boldsymbol{n}_j = \boldsymbol{0} \quad (6)$$

$$\mathcal{F}_i(\boldsymbol{s}_i'') = 0 \quad (7)$$

$$\mathcal{F}_j(\boldsymbol{s}_j'') = 0 \quad (8)$$

where $\mathcal{F}_i$ and $\mathcal{F}_j$ represent the implicit equation of the surfaces and $\boldsymbol{s}_i''$ and $\boldsymbol{s}_j''$ represent the local coordinates of the contact candidate points.

It is important to notice that equation 5 and equation 6 imply the same if equation 4 is verified. As such one of them can be dropped to avoid redundant equations. The system of equations is also easier to solve for internal product conditions rather than for cross product ones. As

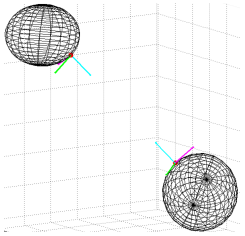

Figure 2: Representation of a pair of candidate contact points and their respective normal (blue), tangent (green) and binormal (magenta) vectors at the correspondent surface.

such:

$$\boldsymbol{n}_i \times \boldsymbol{n}_j = \boldsymbol{0} \Leftrightarrow \begin{cases} \boldsymbol{n}_i \cdot \boldsymbol{t}_j = 0 \\ \boldsymbol{n}_i \cdot \boldsymbol{b}_j = 0 \end{cases} \tag{9}$$

$$\boldsymbol{d}_{ij} \times \boldsymbol{n}_j = \boldsymbol{0} \Leftrightarrow \begin{cases} \boldsymbol{d}_{ij} \cdot \boldsymbol{t}_j = 0 \\ \boldsymbol{d}_{ij} \cdot \boldsymbol{b}_j = 0 \end{cases} \tag{10}$$

where $\boldsymbol{t}_j$ and $\boldsymbol{b}_j$ represent the tangent and binormal vectors of surface j in the considered point of contact. From here on, whenever there is a double prime ($''$) associated with a vector it means that the coordinates of that vector are local.

With equations 7 - 10, the geometric constraints vector $\boldsymbol{c}$ can be defined:

$$\boldsymbol{c} = \begin{bmatrix} \boldsymbol{n}_i \cdot \boldsymbol{t}_j \\ \boldsymbol{n}_i \cdot \boldsymbol{b}_j \\ \boldsymbol{d}_{ij} \cdot \boldsymbol{t}_j \\ \boldsymbol{d}_{ij} \cdot \boldsymbol{b}_j \\ \mathcal{F}_i \\ \mathcal{F}_j \end{bmatrix} \tag{11}$$

In order to use the Newton-Raphson method it is needed to calculate the Jacobian matrix of the constraints vector, which can be given by:

$$\boldsymbol{D}(\boldsymbol{q''}) = \begin{bmatrix} \boldsymbol{t}_j \cdot (\boldsymbol{n}_i)_{\boldsymbol{q''}} & + & \boldsymbol{n}_i \cdot (\boldsymbol{t}_j)_{\boldsymbol{q''}} \\ \boldsymbol{b}_j \cdot (\boldsymbol{n}_i)_{\boldsymbol{q''}} & + & \boldsymbol{n}_i \cdot (\boldsymbol{b}_j)_{\boldsymbol{q''}} \\ \boldsymbol{t}_j \cdot (\boldsymbol{d}_{ij})_{\boldsymbol{q''}} & + & \boldsymbol{d}_{ij} \cdot (\boldsymbol{t}_j)_{\boldsymbol{q''}} \\ \boldsymbol{b}_j \cdot (\boldsymbol{d}_{ij})_{\boldsymbol{q''}} & + & \boldsymbol{d}_{ij} \cdot (\boldsymbol{b}_j)_{\boldsymbol{q''}} \\ \boldsymbol{n}_i'' & & \boldsymbol{0} \\ \boldsymbol{0} & & \boldsymbol{n}_j'' \end{bmatrix} \tag{12}$$

where $\boldsymbol{q''}$ is the vector containing the local coordinates of the contact point for each surface and the subscript $\boldsymbol{q''}$ represents the Jacobian matrix of the vector associated with the subscript.

In order to ensure maximum efficiency for the algorithm, there is a need to easily determine the tangent and binormal vectors of the surface. For that purpose various approaches are possible. In this work, a non-collinear vector $\boldsymbol{u''}$ is used for this:

$$\boldsymbol{t}_j'' = \boldsymbol{n}_j'' \times \boldsymbol{u''} \tag{13}$$

$$\boldsymbol{b}_j'' = \boldsymbol{n}_j'' \times \boldsymbol{t}_j'' \tag{14}$$

The respective Jacobians can be obtained by:

$$\boldsymbol{t}_{\boldsymbol{q''}}'' = \tilde{\boldsymbol{n}}'' \cdot \boldsymbol{u}_{\boldsymbol{q''}}'' - \tilde{\boldsymbol{u}}'' \cdot \boldsymbol{n}_{\boldsymbol{q''}}'' \tag{15}$$

$$\boldsymbol{b}_{\boldsymbol{q''}}'' = \tilde{\boldsymbol{n}}'' \cdot (\tilde{\boldsymbol{n}}'' \cdot \boldsymbol{u}_{\boldsymbol{q''}}'' - \tilde{\boldsymbol{u}}'' \cdot \boldsymbol{n}_{\boldsymbol{q''}}'') - \boldsymbol{n}_{\boldsymbol{q''}}'' \cdot (\tilde{\boldsymbol{n}}'' \cdot \tilde{\boldsymbol{u}}'' - \tilde{\boldsymbol{u}}'' \cdot \tilde{\boldsymbol{n}}'') \tag{16}$$

where $\tilde{\boldsymbol{n}}''$ e $\tilde{\boldsymbol{u}}''$ represent the skew-symmetric matrices of $\boldsymbol{n''}$ e $\boldsymbol{u''}$, respectively.

Once the minimum distance is calculated, it is necessary to determine if there is contact or not. For that we use the value of pseudo-penetration (δ), which can be defined as:

$$\delta = \boldsymbol{n}_j \cdot \boldsymbol{d}_{ij} \tag{17}$$

taking into account that $\boldsymbol{n}_i$ should be a normalized vector. For values of δ higher than zero we consider that there is contact (6).

Once contact is detected, the pseudo-penetration velocity $\dot{\delta}$ needs to be calculated in order to calculate the reaction force. This velocity can be defined as:

$$\dot{\delta} = \frac{d\delta}{dt} = \dot{\boldsymbol{d}}_{ij} \cdot \boldsymbol{n}_j \tag{18}$$

2.3. Force Calculation

In this work the contact force model proposed by Flores *et al.*[21] was implemented. For that model the contact force can be calculated by:

$$F_C = K\delta^n + D\dot{\delta} = K\delta^n + \mathcal{X}\delta^n\dot{\delta} \tag{19}$$

where the value of $\mathcal{X}$ can be determined by:

$$\mathcal{X} = \frac{8K(1-c_r)}{5c_r\dot{\delta^{(-)}}} \tag{20}$$

where $\dot{\delta^{(-)}}$ is the pseudo-penetration velocity immediately before contact.

It is important to notice that for the model implemented, when the coefficient of restitution is 1 the dissipative term is equal to zero, which implies that this force model becomes the purely elastic force model proposed by Hertz [36], and when the coefficient of restitution is 0 the value of $\mathcal{X}$ becomes infinite, which imply a purely plastic contact.

As already stated above, in this work, the friction model implemented consisted in the sum of the Coulomb friction term with a viscous friction term. For that reason, the determination of the friction force the intensity of the contact force is necessary but is not sufficient. It is also required to know the direction and intensity of the velocity tangent to the contact event. This velocity is calculated by having the relative velocity between the points involved in the contact event and the respective pseudo penetration velocity:

$$\boldsymbol{v}_t = \dot{\boldsymbol{d}}_{ij} - \dot{\delta}\boldsymbol{n}_i \tag{21}$$

where $\boldsymbol{v}_t$ is the tangent velocity and $\dot{\boldsymbol{d}}_{ij}$ the relative velocity between bodies.

The intensity of the friction force can be determined as:

$$F_A = \mu_1 F_C + \mu_2 ||\boldsymbol{v}_t|| \tag{22}$$

where μ_1 is the Coulomb friction coefficient and μ_2 is the viscous friction coefficient.

Once known the value of F_A and the direction of $\boldsymbol{v}_t$ all that remains is to calculate the corresponding vector:

$$\boldsymbol{F}_A = F_A \hat{\boldsymbol{v}}_t \tag{23}$$

where $\hat{\boldsymbol{v}}_t$ represents the tangent velocity direction.

By looking at equation 23 is possible to see that the friction force is different than zero only when there is a tangent velocity different than zero. However, as this velocity tends to zero, the norm of the friction force does not end to zero but to $\mu_1 F_C$, which is at least $\mu_1 P$, where P is the force associated with the gravity (when the body is in contact with a surface but in rest). This means that soon as the tangent velocity is different than zero, but still small enough that the second term of equation 23 could be assumed zero, the friction force becomes the value above described. For $\hat{\boldsymbol{v}}_t = \boldsymbol{0}$ it is zero. This means that the model applied has a discontinuity near $||\boldsymbol{v}_t|| = 0$.

Because in the integration process discontinuities will lead to instability (and possible divergence), it is necessary to make an approximation for tangent velocity values near zero so that it becomes continuous. For the velocities for which the approximation is valid, the friction force is given by:

$$F_A = (\frac{\mu_1 F_C}{v_0} + \mu_2)\frac{||\boldsymbol{v}_t^*||}{v_0}||\boldsymbol{v}_t|| \tag{24}$$

where v_0 is a threshold for the tangent velocity below which the approximation is to be valid and $||\boldsymbol{v}_t^*||$ is the approximation made for the velocity according to equation 25:

$$||\boldsymbol{v}_t^*|| = (k_3||\boldsymbol{v}_t||^3 + k_2||\boldsymbol{v}_t||^2 + k_1||\boldsymbol{v}_t|| + k_0)v_0 \tag{25}$$

In order to ensure that the function obtained with the approximation is a continuous function, the values for k_3, k_2, k_1 and k_0 were determined to be:

$$k_3 = -\frac{2}{v_0^3} \tag{26}$$

$$k_2 = \frac{\mu_2}{(\mu_1 F_C + \mu_2 v_0)v_0} + \frac{2}{v_0^2} \tag{27}$$

$$k_1 = -\frac{\mu_2}{\mu_1 F_C + \mu_2 v_0} - \frac{1}{v_0} \tag{28}$$

$$k_0 = 0 \tag{29}$$

2.4. Contact detection and Force model Validation

Before these models could be applied to human gait, it was necessary to ensure that the results produced would be correct. For that reason, simple tests cases were used (bouncing ball, newton cradle and an ellipsoid rolling down an inclined plane). The results from these simple test showed that the model was producing the expected results.

One of the most important results of this validation is presented in figure 3. The force model implemented was compared with the models proposed by Hunt and Crossley and by Lankarani and Nikravesh [21]. Various simulations were made, all with different coefficients of restitution, in order to compare the coefficients of pre- and post-restitution.

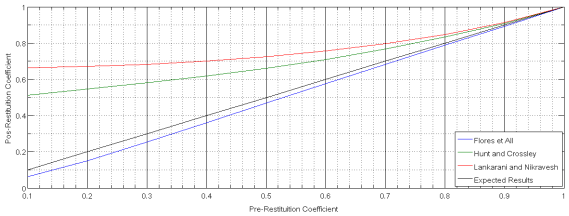

Figure 3: Variation of the coefficient of post-restitution with the coefficient of pre-restitution

The results obtained are in accordance with what was expected for the models considered, which implies that the detection method and the contact models are correctly implemented.

2.5. Optimization

As described above, during this work different approaches were used and because of that two different functions were considered as objectives of the optimization problem: one scalar, which led to a single objective optimization, and a vector, which led to a multi-objective optimization. As the purpose of this work is to measure foot ground contact accurately, the function to be minimized has to include the absolute value of the force residual and the absolute value of the point residual. The force residual can be defined as the difference between the values of the forces measured experimentally and the forces calculated by the model. In the same way, the point residual is the difference between the application point measured and the application point calculated by the model.

For both cases, scalar and vectorial objective function, the value to be minimized is the maximum residual, that is, the higher value of the residual for all the time steps considered.

In order to account for differences in all three directions, for each time step the sums of the force and applications points residuals in the three directions are considered.

The scalar objective function considered needs to account for both residuals. As such when written mathematically, the scalar objective function corresponds to the weighted sum of the force and application point residuals (summed in all three components) and is given by:

$$f = \max(\sum_{j=1}^{3} \omega_1|(F_j - F_j^*)| + \omega_2|(P_j - P_j^*)|) \tag{30}$$

where F and P correspond to the forces and application point calculated by the model, F^* and P^* correspond to the forces and application point determined experimentally and j corresponds to the direction considered (x, y or z). ω_1 and ω_2 are the weights that each term of the sum has

for the over all objective function. For this function it is also important that the residuals are normalized, i.e., that the order of magnitude of each residual is the same.

On the other hand, a vectorial objective function does not require weights for each residual or normalization as their are considered in different axis for the evaluation. This multi-objective function can by given by:

$$f = \begin{bmatrix} \max(\sum_{j=1}^{3} |(F_j - F_j^*)|) \\ \max(\sum_{j=1}^{3} |(P_j - P_j^*)|) \end{bmatrix} \quad (31)$$

The experimental data obtained in terms of ground reaction forces and application points corresponds to a single force and application point, while the model produces as many forces and application points as the number of surfaces used to describe the body. For that reason, it is necessary to "treat" the data form the model in such way that a single force and application point are obtained. In terms of forces it is possible to use the concept of resultant force in order to obtain a single force from all the forces calculated by the model:

$$\boldsymbol{F}_R = \sum_{i=1}^{ncp} \boldsymbol{F}_i \quad (32)$$

where $\boldsymbol{F}_R$ is the resultant force, $\boldsymbol{F}_i$ is the force for the surface i and ncp represents the number of contact pairs of the model.

However the solution for the application point is not so simple. The application point needs to be calculated in such a way that the sum of the moments resultant from each force is equal to the moment generated by the resultant force [25]. As such the resultant application point is given by:

$$\boldsymbol{P}_R = \tilde{\boldsymbol{F}_R}^{-1} \cdot \sum \boldsymbol{F}_i \times \boldsymbol{P}_i \quad (33)$$

where $\boldsymbol{m}_R$ is the resultant moment, $\boldsymbol{m}_i$ is the moment of the i^{th} surface, $\boldsymbol{P}_R$ is the resultant application point, $\boldsymbol{P}_i$ is the i^{th} application point and $\tilde{\boldsymbol{F}_R}$ represents the skew-symmetric matrix originated from the resultant force vector.

For this optimization process thirteen variables were considered for each surface on the foot: a, b, c (ellipsoid axis), r_x, r_y, r_z (ellipsoid position), α, β, γ (ellipsoid orientation), K, cr (contact parameters), μ_1 and μ_2 (friction parameters). The constraints used for each variable were chosen in such a way that in the first time step of the analysis there would be no contact.

The optimization process was implemented in Matlab® and resorting to its built-in optimization routines. These routines produce sets of values for the variables to be optimized, for which the value of the objective function is calculated. However, in this optimization process, it is necessary to use software external to Matlab (Apollo), in order to "transform" the parameters introduced by the optimizer into forces and application points.

In a first approach for the optimization process, the optimizer function $fmincon$ was used. This function tries to find the minimum of a user defined function, respecting the constraints defined by the user. The user defined function, for which the optimizer tried to find a minimum, correspond to the above described scalar objective function.

In terms of validation, this approach produced good results for situations where the starting point was the correct solution of the problem. However, once some of the values of this initial approximation were changed, the results were less satisfactory, leading to a change in the optimization process.

For a second approach to the optimization process genetic algorithms were used. These algorithms are based in the concept that individuals that have adapted better to the environment requirements are more probable to survive. As such, their genes are frequently passed down to generations, improving the average fitness of the population. The implementation of this concept to optimization processes can be made considering that individuals represent sets of values for the parameters to be optimized and that the adaptation of those individuals is translated into an evaluation of a fitness function (correspondent to the previously referred objective function). The evolutionary process is then applied for creating better sets of values for the parameters of the problem [37].

In these algorithms each generation fitness is evaluated and a new generation is created based in the previous generation. The way this new generation is created is though the reproduction and mutation of some of the best individuals of the previous generation. Also, in some cases, the elite (the best of the best individuals) of the previous generation can be passed to the next without any change [37].

In this approach of the problem, a multi-objective genetic algorithm (from Matlab) was used. For that the fitness function used was the vectorial objective function defined in equation 31. It is important to refer that while optimization processes with a single objective function produce a single best solution, multi-objective algorithms produce various solutions, each representing a trade-off in terms of values for each of the objective functions. These various solution normally correspond to the *Pareto Front*, which can be defined as the set of solutions for which it is not possible to improve the value of one of the objective functions without worsen other [38].

The complexity of any optimization problem is increased as the number of variables increases. For those reasons it is more efficient to divide the problem in two different stages: the first a smaller problem, with less variables and the second the full problem, where the initial population is defined as the solutions obtained from the smaller problem.

This approach was used directly in the surfaces used to describe the foot, first approximated as spheres and then with the freedom of changing into ellipsoids with a given orientation.

3. Results

The results were obtained in two different ways: from the optimization process and from manually choosing parameters for the surfaces in a trial and error process. The results presented for the optimization are preliminary results, since due to the high complexity of the problem, the process is still running.

3.1. Manually chosen Parameters

Due to the optimization process implemented being an expensive process, both computationally and in terms of time, the values for the parameters that could lead to a good approximation of the forces and application point were found in a manual approximation, that is, though a trial and error process. The values found are presented in table 2.

Table 2: Manually obtained values for the parameters

Surface	1	2	3	4	5
K	1.5e4	1.0e4	3.0e4	1.0e4	3.2e5
cr	0.9	0.9	0.9	0.9	0.9
μ_1	0.6	0.6	0.7	0.6	0.05
μ_2	0.0	0.0	5.0	5.0	15.0
a	0.03	0.022	0.02	0.06	0.025
b	0.02	0.043	0.055	0.025	0.04
c	0.014	0.014	0.012	0.01	0.009
r_x	0.02	0.02	0.08	0.03	-0.04
r_y	0.04	-0.015	0.009	-0.01	0.02
r_z	-0.03	-0.025	-0.02	-0.02	0.0
α	-10	-10	-10	-10	-10
β	5	5	-2	-2	25
γ	0	-45	0	0	0

These values were found based on the graphical differences between the forces originated by the model implemented and the forces measured in the force plates during gait. A comparison between the different components of these forces is presented in figure 4, figure5 and figure 6.

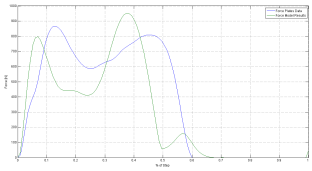

Figure 4: Comparison between the vertical component of the forces experimentally obtained with the ones calculated by the model.

From the observation of figure 4 and figure 5 it is seen that a reasonable approximation of the vertical and lateral/medial forces was obtained. A good approximation of the anterior posterior force was not achieved. In previous works of biomechanical models of the foot with ground interaction, a good approximation of the vertical component is commonly obtained. However, when compared with the results in bibliography, the results obtained for the vertical

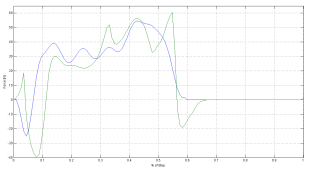

Figure 5: Comparison between the lateral/medial component of the forces experimentally obtained with the ones calculated by the model.

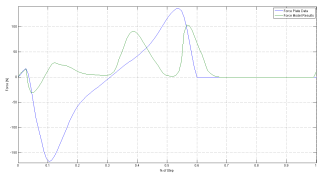

Figure 6: Comparison between the anterior/posterior component of the forces experimentally obtained with the ones calculated by the model.

force are not as good, that is, present a higher error when compared with the measurements from the force plates [27, 32]. The reasons behind this higher error could be the smaller number of surfaces used to describe the sole of the foot or the fact that the number and position of the surfaces was chosen not to correctly approximate the actual surface that describes the sole of the foot, but rather in function of the pressure distribution felt in the foot during gait. Moreira obtains better results for the vertical force by using nine spheres of different radius, that closely approximate the sole of the foot [27]. On the other hand, Vilà uses a model with only four spheres which also closely approximate the vertical force. However, instead of a computational trial and error process to place those spheres, an optimization algorithm was used [32].

Looking at the remaining ground reaction forces, obtaining a good approximation for the lateral/medial and anterior posterior components of the ground reaction force is not as common [27, 32, 39]. Once again, for obtaining this approximation, a trial and error approach was used. The tuning of the friction constants that are responsible for this forces was only made after the approximation of the vertical force was considered acceptable. This tuning of the friction constants allowed for an acceptable approximation for the lateral/medial ground reaction force, but not for the anterior/posterior force. The fact that acceptable results were not obtained for the anterior/posterior force were not obtained may be related with the fact that there was not much similarity between the application points in the direction of that force.

3.2. Parameters Obtained Though Optimization

Even though it was tried to find good parameters for this problem, through a trial and error process, the optimization process was also run. Because the optimization process is more exhaustive in looking for a solution is is probable that it will find a better solution than the one obtained above. However, because it is a costly process, at the time of the submission of this work only results for the first stage of the optimization process (that used the maximum of the residuals as objective function) are available. For the second stage of this optimization and for the first stage of the optimization that used the time sum of the residuals only "preliminary" results are available.

For all the optimization processes run in this work, the shape of the Pareto front was saved in different generations so that their evolution could be gauged. For the first stage of the optimization process that used the maximum of the residuals as objective function, the fronts obtained are presented in figure 7.

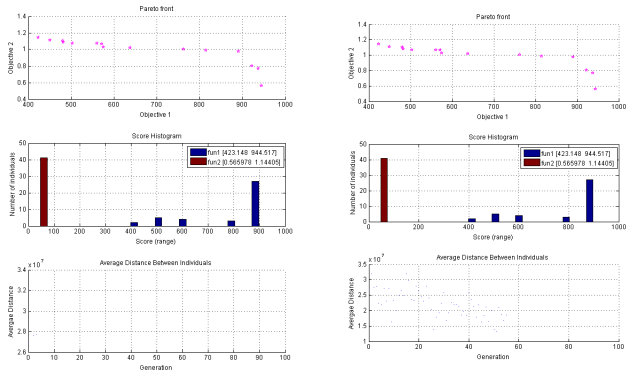

Figure 7: Optimization results for the first stage after three generations (left) and after fifty five generations (right). (Top) Pareto Front. (Middle) Score distribution. (Bottom) Average distance between the individuals of each generation.

In the above figure, some of the points that make up the Pareto front, in two times of the optimization are presented. By comparing the Pareto fronts presented and the scores distribution, it can be seen that the results after three generations are the same as the ones after fifty five generations. This is the exact opposite from what was expected, since as the optimization progresses the Pareto front should change and approximate an hyperbole. These results can be justified by the fact that this optimization was stopped after one generation to introduce some corrections and when it was restarted the "results" from the first generation were given as part of the initial population. When running an optimization, only a percentage (defined by the user) of the actual front is plotted and given as a solution. It is possible that by introducing as an initial population the exact fraction of the Pareto front that is kept for plotting, that fraction remains unchanged. This also could indicate that the initial values tested were actually the best possible values, although that would be statistically very unlikely. However, as the front was not evolving, this optimization was stopped an the results were used as a part of the initial population of the next stage of the optimization. Looking at the average distance between the individuals of each generation, it can be seen that this presents a tendency to decrease. This was expected as as the optimization progresses, the individuals should be getting closer to each other and to the solution.

In order to evaluate the effectiveness of this stage, the results corresponding to the extremes of the Pareto front were compared. Figure 8 presents the forces obtained for those points.

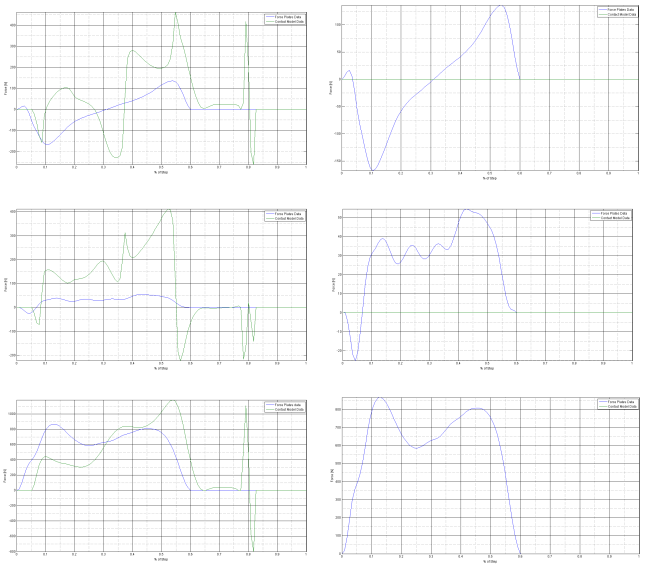

Figure 8: Force Results for the extreme values of the Pareto Front. (Top) Anterior Force. (Middle) Lateral Force. (Bottom) Vertical Force. (Left) Minimum of objective 1 and Maximum of Objective 2. (Right) Maximum of objective 1 and Minimum of Objective 2

From the results presented in the figure 8, it is possible to observe that the approximations of the forces of the best and worst situation of objective function 1 (that corresponds to the force residuals) are not the best. Also, looking at the values of each objective function, it can be seen that the errors for the forces and application points (objective one and two, respectively) are considerably high. A first justification for this can be the fact that the Pareto front did evolve as the generations passed, possible due to an error of the set up of the problem.

Another possible justification to the high values of objective functions can be the fact that at this stage, only spheres are being considered. As such, and because only five surfaces are being considered, it might be harder to find parameters that correspond to a low evaluation of the fitness function, as spheres are less "flexible" surfaces, when compared to ellipsoids.

Lastly, the parameters bounds might also be too tight

in order for the optimizer to find a good solution. These bounds were chosen so that if there was an individual which parameters were all the lower bound values or the upper bound values, there would be no contact at the first time step of the analysis. Because the force model requires the value of the pre-contact velocity in order to calculate the force (Eq.(20)), if in the first time step there is already contact, the force obtained will by infinite.

As stated above, and even though the results obtained for this first stage were worse than expected, the solution obtained was used as a partial initial population for the second stage of the optimization process (where the surfaces are allowed to change from spheres to ellipsoids). At the time of delivering this work, this stage has yet to finish. However, as for the previous stage, it is possible to compare the Pareto front, the score diversity and the average distance after a different number of generations. Figure 9 shows the Pareto front and other results after thirty eight generations.

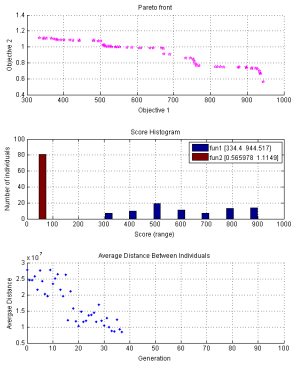

Figure 9: Optimization results for the second stage after thirty eight generations. (Top) Pareto Front. (Middle) Score distribution. (Bottom) Average distance between the individuals of each generation.

Looking to figure 9 and comparing the Pareto front or the score distribution to the ones obtained at the end of the first stage, a clear improvement can be observed.

One aspect that is important to notice is that the maximum and minimum of the objective function 1 decrease significantly, which is what was wanted and expected. Also. once again is observed a decreasing tendency in the average distance which means the point that constitute the population are getting closer.

4. Conclusions

The results obtained from this work for human gait were sets of values for the position, size, orientation and contact constants for each surface, and the forces generated were compared with the ones acquired from force plates. Two approaches were used: one based on a trial and error process and other based on the optimization process described. The results from the trial and error process show a good similarity for the lateral component of the ground reaction force and a reasonable approximation of the vertical force. The results for the anterior component were very different than what was measured in the force plate. Not having achieved a better approximation of the vertical force, without trying all possible combination of values for the parameters considered, supports the need of an optimization process. It was considered that adding more surfaces based on the graphical distribution could be beneficial. However since the optimization process running was only considering five surfaces and with a comparison between the results obtained from both methods in mind, more surfaces were not added.

At the time of the end of this work, the full optimization process was not yet finished, due to being very time consuming. However, the results form the first stage of the maximum residual optimization were presented. The values for the objective functions presented in this front were relatively high. The forces originated by the parameters tested from the front obtained were very different from the experimental forces. That can be justified by being the first stage of the process. However, by limiting the surfaces in terms of shape (only spheres are allowed) it is possible that the values of the objective functions for the results of this first part are not as low as it would be expected for an optimization process. Also, it is possible that the values used as upper and lower bounds restrict, more than needed, the possible values that the parameters could assume, which can also have an impact on the results. The front obtained for the second stage of the optimization is promising in terms of the final results to be obtained.

References

[1] SJ Hall. *Basic Bimechanics*. McGraw-Hill, Delaware, 6th edition, 2012.

[2] Tung Wu Lu and Chu Fen Chang. Biomechanics of human movement and its clinical applications. *Kaohsiung J. Med. Sci.*, 28(2 SUPPL.):S13–S25, 2012.

[3] A Lees. Biomechanics applied to soccer skills. In *Sci. Soccer*, chapter 12. Routledge, 3rd edition, 2013.

[4] Peter Dabnichki. Biomechanical testing and sport equipment design. *Sport. Eng.*, pages 93–105, 1998.

[5] Tiago Malaquias. *Development of a Three-Dimensional Multibody Model of the Human Leg and Foot for Application to Movement Analysis*. PhD thesis, Instituto Superior Tecnico, 2013.

[6] Daniel S. Lopes, Miguel T. Silva, Jorge a. Ambrósio, and Paulo Flores. A mathematical framework for rigid contact detection between quadric and superquadric surfaces. *Multibody Syst. Dyn.*, 24(3):255–280, September 2010.

[7] S Kockara, T Halic, and C Bayrak. Contact Detection Algorithms. *J. Comput.*, 4(10):1053–1063, 2009.

[8] Juhwan Choi, Han Sik Ryu, Chang Wan Kim, and Jin Hwan Choi. An efficient and robust contact algorithm for a compliant contact force model between bodies of complex geometry. *Multibody Syst. Dyn.*, 23(1):99–120, 2010.

[9] H Cenk Güler, Necip Berme, and SR Simon. A viscoelastic sphere model for the representation of plantar soft tissue during simulations. *J. Biomech.*, 31:847–853, 1998.

[10] Brian Mirtich. Rigid body contact: Collision detection to force computation. *Work. Contact Anal. Simulation, IEEE . . .*, 1998.

[11] Pedro Moreira, Paulo Flores, and Miguel Silva. A biomechanical multibody foot model for forward dynamic analysis. *2012 IEEE 2nd Port. Meet. Bioeng. ENBENG 2012*, 2012.

[12] Ming C. Lin, Dinesh Manocha, Jon Cohen, and Stefan Gottschalk. Collision Detection: Algorithms and Applications. 1996.

[13] Gerhard Hippmann. An Algorithm for Compliant Contact Between Complexly Shaped Surfaces in Multibody Dynamics. *Multibody Dyn. Jorge AC Ambrosio (Ed.), IDMEC/ . . .*, pages 1–19, 2003.

[14] Yi King Choi, Jung Woo Chang, Wenping Wang, Myung Soo Kim, and Gershon Elber. Continuous collision detection for ellipsoids. *IEEE Trans. Vis. Comput. Graph.*, 15(2):311–324, 2009.

[15] Xiaohong Jia, Yi King Choi, Bernard Mourrain, and Wenping Wang. An algebraic approach to continuous collision detection for ellipsoids. *Comput. Aided Geom. Des.*, 28(3):164–176, 2011.

[16] Christian Wellmann, Claudia Lillie, and Peter Wriggers. A contact detection algorithm for superellipsoids based on the common-normal concept. *Eng. Comput.*, 25(5):432–442, 2008.

[17] D.S. Lopes, M.T. Silva, and J.a. Ambrósio. Tangent vectors to a 3-D surface normal: A geometric tool to find orthogonal vectors based on the Householder transformation. *Comput. Des.*, 45(3):683–694, March 2013.

[18] Janete Alves, Nuno Peixinho, Miguel Tavares da Silva, Paulo Flores, and Hamid M. Lankarani. A comparative study of the viscoelastic constitutive models for frictionless contact interfaces in solids. *Mech. Mach. Theory*, 85:172–188, March 2015.

[19] J Choi, Sungsoo Rhim, and JH Choi. A general purpose contact algorithm using a compliance contact force model for rigid and flexible bodies of complex geometry. *Int. J. Non. Linear. Mech.*, 53:13–23, July 2013.

[20] Margarida Machado, Pedro Moreira, Paulo Flores, and Hamid M. Lankarani. Compliant contact force models in multibody dynamics: Evolution of the Hertz contact theory. *Mech. Mach. Theory*, 53:99–121, 2012.

[21] Paulo Flores, Margarida Machado, Miguel T Silva, and Jorge M Martins. On the continuous contact force models for soft materials in multibody dynamics. *Multibody System Dynamics*, 25(3):357–375, 2011.

[22] H. Olsson, Kj K.J. Å ström, C. Canudas de Wit, M. Gäfvert, and P. Lischinsky. Friction Models and Friction Compensation. *Eur. J. Control*, 4(3):176–195, 1998.

[23] Ej Berger. Friction modeling for dynamic system simulation. *Appl. Mech. Rev.*, 55(6):535, 2002.

[24] V Van Geffen. A study of friction models and friction Compensation. Technical report, Technische Unicersiteit Eindhoven, Eindhoven, 2009.

[25] David A Winter. *Biomechanics and motor control of human gait: normal, elderly and pathological*. 1991.

[26] Yves Gonthier, John McPhee, Christian Lange, and Jean-Claude Piedbœ uf. A Regularized Contact Model with Asymmetric Damping and Dwell-Time Dependent Friction. *Multibody Syst. Dyn.*, 11(3):209–233, April 2004.

[27] Pedro Filipe da Silva Moreira. *Development of a three-dimensional contact model for the foot ground interaction in gait simulations*. PhD thesis, Universidade do Minho, 2009.

[28] R.J Abboud. (i) Relevant foot biomechanics. *Curr. Orthop.*, 16(3):165–179, 2002.

[29] L. a. Gilchrist and D. a. Winter. A two-part, viscoelastic foot model for use in gait simulations. *J. Biomech.*, 29(6):795–798, 1996.

[30] Dwight Alan Meglan. *Enhaced Analysis of human locomotion*. PhD thesis, The Ohio State Univesity, 1991.

[31] T. R. Jenkyn and a. C. Nicol. A multi-segment kinematic model of the foot with a novel definition of forefoot motion for use in clinical gait analysis during walking. *J. Biomech.*, 40(14):3271–3278, 2007.

[32] Rosa Pàmies Vilà. *Application of Multibody Dynamics Techniques to the Analysys of Human Gait*. PhD thesis, Universitat Politècnica de Catalunya, 2012.

[33] Roger Fletcher. *Practical methods of optimization*. John Wiley & Sons, 2013.

[34] Jorge Nocedal and Stephen Wright J. *Numerical Optimization*, volume 2nd. 2006.

[35] Daniel S. Lopes. *Smooth convex surfaces for modeling and simulating multibody systems with compliant contact elements*. PhD thesis, Instituto Superior Técnico, 2013.

[36] Heinrich Rudolf Hertz. On the contact of solids - on the contact of rigid elastic solids and on hardness. In *Misc. Pap.*, volume 92, pages 146–183. Macmillian and Co., London, 1896.

[37] Alexander K. Hartmann and Heiko Rieger. *Optimization Algorithms in Physics*, volume 11. Wiley, 2010.

[38] David A Van Veldhuizen and Gary B Lamont. Evolutionary computation and convergence to a pareto front. In *Late breaking papers at the genetic programming 1998 conference*, pages 221–228. Citeseer, 1998.

[39] Miguel Pedro Tavares da Silva. *Human motion analysis using multibody dynamics and optimization tools*. PhD thesis, 2003.